First Seismic Receiver Functions on the Moon

Hugues Chenet[(1)], Lev P. Vinnik[(2)], Jeannine Gagnepain-Beyneix[(1)], Philippe Lognonné [(1)]

chenet@ipgp.jussieu.fr

(1) Département des Études Spatiales, Institut de Physique du Globe de Paris, France

(2) Institute of Physics of the Earth, Moscow, Russian Federation

Introduction

The Apollo Seismic network (4 stations) was installed on the near side of the Moon between 1969 and 1972. Recordings stopped in 1977. It provided the only seismic data set available to study extraterrestrial planet interior. Our study of lunar seismic recordings is very different from those previously used in lunar exploration. It is based on the S receiver function technique (*Farra and Vinnik, 2000*) which analyses phase conversions on discontinuities beneath the station.

Lunar Seismology

Seismic propagation features and seismic activity on the Moon are described in details by *Toksöz et al. (1974), Lammlein et al. (1974)* and *Lognonné and Mosser (1993).*

- Seismologic events:
  - Meteoritic and artificial impacts (ascent stage of Lunar Modules and *Saturn* third-stage booster (S4B))
  - Superficial High Frequency Teleseismic Events (thermo-elastic cooling)
  - Deep Events (periodic, thousands of recorded events, localised in 52 focus)
- Seismologic properties:
  - Very low noise level
  - Very weak attenuation on surface
  - High scattering superficial layer

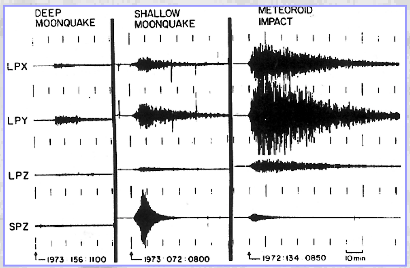

Data

We use recordings of deep moonquakes. They are extremely weak but events originating from a given location match together in nearly every detail for their entire duration. This similarity allows to enhance their amplitude by stacking up to 50 records of every group of seism.

Method

We look for the secondary phases related to **SV** waves but arriving at the receiver as **P** waves. **Sp** phase is formed by conversion from **S** to **P** at discontinuities beneath the station. The **SV** waves of deep seismic events are polarized practically in the radial (R) direction. Secondary phases arriving at the surface as **P** waves should be present practically only in the vertical (Z) component.

•We deconvolve the R and Z components of each record by the R component of the **S** wave. Deconvolution is performed in time domain with a proper regularization. The deconvolution filter is calculated in time windows of 15-20 seconds. In the deconvolved R component the **S** wave looks as a "bump" (Fig.❶). The deconvolution transforms into standard form the secondary phases (Fig.❷), and they can be detected by stacking the records of many seismic events with appropriate moveout time corrections (Fig.❸).

❶
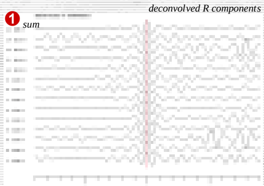

❷
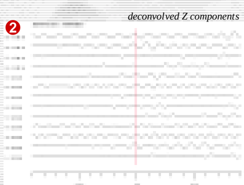

•The expected time interval between the secondary phase and **S** in first order approximation is a linear function of the ray parameter of the **S** wave. To detect these phases, the deconvolved Z components are stacked with moveout time corrections : the correction for the record with a ray parameter p_1 is calculated as $a(p_1 - p_0)$, where p_0 is the average value of p for the given set of records. The stacked Z components are shown in Figure 4. The different traces are obtained for values of a between -0.02 and 0.02. Origin of the time scale is the same as in Figure ❶.

To interpret the data in Figure ❸, they are compared with theoretical seismograms for plane waves propagating from the half space through the stack of plane isotropic layers. For the incoming **SV** wave, the spectra of the R and Z components at the free surface are related via the corresponding transfer functions $H_R(\omega)$ and $H_Z(\omega)$ as:

$$Z(\omega) = R(\omega) * \frac{H_Z(\omega)}{H_R(\omega)} \qquad (1)$$

We calculate the transfer functions for the given model with the algorithm by Haskell (1962). The sum of the deconvolved R components is used as an input. Z(ω) is obtained via Eq. (1), and the corresponding function of time is obtained by inverse Fourier transformation. We calculate the theoretical Z components for the slowness values of the actual seismograms, and then stack them like the real seismograms.

Results

Figure ❼ and Figure ❽ show the stacks of the synthetic Z components for our two models (mod1 and mod2 in Fig.❺), obtained by modifying the uppermost layer of *Toksöz (1974)* model (Fig. ❹❺❻), often used as a reference crust model. Both theoretical and observed stacks contain M-shaped phases which arrives at about -8 sec.(label 1) and -0.4 sec.(label 2) before the main S arrival (time=0). This is ***Sp*** phase respectively from the mantle-crust transition and the bottom of the superficial low-velocity layer. Second "bumps" in the specific M-shape are caused by reverberation in the shallow layer.

Our two different models propose faster velocities in the first kilometer. Both models are equivalent in comparison to the data.

❹
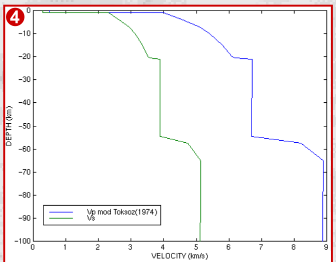

Seismic velocity reference model from *Toksöz (1974)*

❻
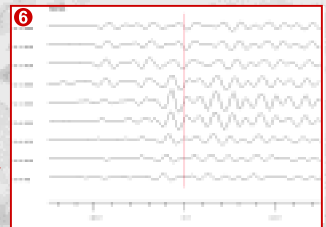

Stacks for model of *Toksöz (1974)*

❸
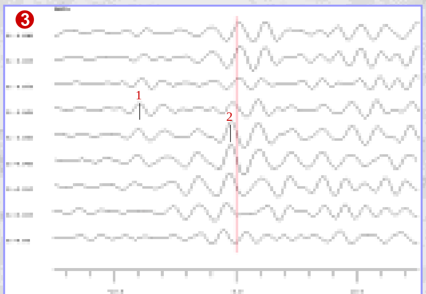

Stacks of deconvolved Z components with different moveout corrections

❼
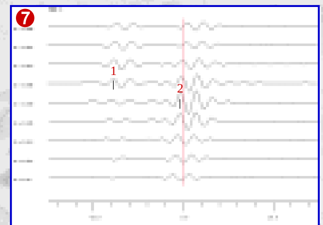

Stacks for model mod1

❺
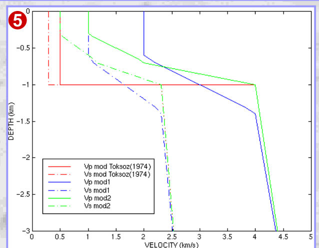

Different models used to compute synthetics. Zoom on the upper crust

❽
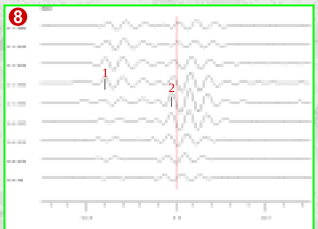

Stacks for model mod2

Conclusion

Our analysis shows that average seismic velocities in the upper layer of the crust at station 12 are higher than in Toksöz model. The optimum model is not unique. The synthetics for an acceptable model must contain the ***sP*** phase from the base of the low-velocity layer with a lead time around 0.4 sec. relative to **S**. This can be obtained by increasing the velocities and also by reducing the thickness of the layer, relative to the reference model (*Toksöz, 1974*). Moreover our data imply a good seismic transparency for the crust bellow station 12, whereas the method didn't work at other stations. This can result from a thinner or/and less fractured upper crust than usually assumed. Time, amplitude and waveform of ***Sp*** phase from the mantle-crust boundary are very similar between data and our synthetics. Thus the data lends support to reference model with modified superficial layer. Nevertheless, other models may exist that fit the data equally well.

References

Farra V. and L.P. **Vinnik**, Upper mantle stratification by P and S receiver functions, *Geophys. J. Int.*, **141**,p. 669-712, 2000.

Goins, N. R., A. M. Dainty et M.N. Toksöz, Lunar seismology : the internal structure of the Moon, *JGR*, **86**, p.5061-5074, 1981a.

Haskell, N. A., Crustal reflection of P and SV waves, *J. Geophys. Res.*, **67**, p.4751-4767, 1962.

Lammlein, D., G. Latham, J. Dorman, Y. Nakamura et M. Ewing, Lunar seismicity, structure and tectonics, *Rev. Geoph. Space Physics*, **12**, p.1-21, 1974.

Lognonné, P. et B. **Mosser**, Planetary Seismology, *Surveys in Geophysics*, **14**, p.239-302, 1993.

Nakamura, Y., Seismic velocity structure of the lunar mantle, *JGR*, **88**, p.677-686, 1983.

Toksöz, M.N., A. M. Dainty, S.C. Solomon et K.R. Anderson, Structure of the Moon, *Rev. Geoph. Space Physics*, **12**, p.539-567, 1974.